

# *Local and remote impacts of aerosol species on Indian summer monsoon rainfall in a GCM*

Article

Published Version

Creative Commons: Attribution 4.0 (CC-BY)

Open access

Guo, L., Turner, A. G. ORCID: <https://orcid.org/0000-0002-0642-6876> and Highwood, E. J. (2016) Local and remote impacts of aerosol species on Indian summer monsoon rainfall in a GCM. *Journal of Climate*, 29 (19). pp. 6937-6955. ISSN 1520-0442 doi: <https://doi.org/10.1175/JCLI-D-15-0728.1>  
Available at <https://centaur.reading.ac.uk/44562/>

It is advisable to refer to the publisher's version if you intend to cite from the work. See [Guidance on citing](#).

To link to this article DOI: <http://dx.doi.org/10.1175/JCLI-D-15-0728.1>

Publisher: American Meteorological Society

All outputs in CentAUR are protected by Intellectual Property Rights law, including copyright law. Copyright and IPR is retained by the creators or other copyright holders. Terms and conditions for use of this material are defined in the [End User Agreement](#).

[www.reading.ac.uk/centaur](http://www.reading.ac.uk/centaur)

**CentAUR**

Central Archive at the University of Reading

Reading's research outputs online

## Local and Remote Impacts of Aerosol Species on Indian Summer Monsoon Rainfall in a GCM

LIANG GUO AND ANDREW G. TURNER

*National Centre for Atmospheric Science, and Department of Meteorology, University of Reading, Reading, United Kingdom*

ELEANOR J. HIGHWOOD

*Department of Meteorology, University of Reading, Reading, United Kingdom*

(Manuscript received 15 October 2015, in final form 24 June 2016)

### ABSTRACT

The HadGEM2 AGCM is used to determine the most important anthropogenic aerosols in the Indian monsoon using experiments in which observed trends in individual aerosol species are imposed. Sulfur dioxide (SD) emissions are shown to impact rainfall more strongly than black carbon (BC) aerosols, causing reduced rainfall especially over northern India. Significant perturbations due to BC are not noted until its emissions are scaled up in a sensitivity test, resulting in rainfall increases over northern India due to the elevated heat pump mechanism, enhancing convection during the premonsoon, and bringing forward the monsoon onset. Second, the impact of anthropogenic aerosols is compared to that of increasing greenhouse-gas concentrations and observed sea surface temperature (SST) warming. The tropospheric temperature gradient driving the monsoon shows weakening when forced by either SD or imposed SST trends. However, the observed SST trend is dominated by warming in the deep tropics; when the component of SST trend related to aerosol emissions is removed, further warming is found in the extratropical Northern Hemisphere that tends to offset monsoon weakening. This suggests caution is needed when using SST forcing as a proxy for greenhouse warming. Finally, aerosol emissions are decomposed into those from the Indian region and those elsewhere in pairs of experiments with SD and BC. Both local and remote aerosol emissions are found to lead to rainfall changes over India; for SD, remote aerosols contribute around 75% of the rainfall decrease over India, while for BC the remote forcing is even more dominant.

### 1. Introduction

More than a billion people in South Asia rely on the monsoon to supply over 80% of annual rainfall between June and September. Pressure on water resources is increasing, owing to the rapidly rising population and its need for industrial development, personal water supply,

and rainfed or irrigated agriculture. Thus, understanding how monsoon rainfall is changing under anthropogenic forcing is vital for planning investment in infrastructure and for food and water security. At the same time, industrial development, growth of private vehicle transportation, and continued use of home-cooking fires is leading to large increasing trends in regional emissions of precursors to sulfate aerosols and black carbon (BC) (Kaskaoutis et al. 2012; Babu et al. 2013). These are particularly concentrated in the Indo-Gangetic plains (IGP) region, pushed up against the Himalayan foothills (Lau et al. 2006) where they can affect weather and climate as well as human health. Aerosol emissions elsewhere in the Northern Hemisphere also increased in the early and mid-twentieth

Denotes Open Access content.

Supplemental information related to this paper is available at the Journals Online website: <http://dx.doi.org/10.1175/JCLI-D-15-0728.s1>.

*Corresponding author address:* Liang Guo, Department of Meteorology, University of Reading, Earley Gate, P.O. Box 243, Reading RG6 6BB, United Kingdom.  
E-mail: l.guo@reading.ac.uk



This article is licensed under a [Creative Commons Attribution 4.0 license](https://creativecommons.org/licenses/by/4.0/).

century, but European and U.S. emissions have declined since the 1980s, following air quality legislation. Thus, it is important to understand the likely impact of changes in the amount and spatial pattern of emissions on the South Asian monsoon climate.

Long records of gauge-based observations over India dating back to the 1870s reveal considerable decadal variations and long-term trends in the Indian monsoon (e.g., [Turner and Annamalai 2012](#); [Krishnamurthy and Goswami 2000](#)). Several studies have noted overall negative trends: [Ramanathan et al. \(2005\)](#) found negative trends particularly in July up to 2000, while, with data up to 2004, [Gautam et al. \(2009\)](#) found significant declining trends from July to September over India. However, other studies of rainfall characteristics at the local and regional scales have noted decreases in the frequency of light-to-moderate rainfall and an increased number of extreme heavy rainfall events, leading to little trend in the seasonal rainfall total ([Goswami et al. 2006](#); [Dash et al. 2009](#)). Recent comparisons of trends in two and four different gridded datasets for India noted area-averaged rainfall decreases since the 1950s [[Krishnan et al. \(2013\)](#) and [Bollasina et al. \(2011\)](#), respectively], although with considerable spatial uncertainty (especially in northeastern peninsular India); relatively few grid points show statistically significant trends. The recent study of [Roxy et al. \(2015\)](#) has demonstrated a significant negative trend in rainfall over northern India since 1900.

The observed decrease in rainfall is not what would be expected from the response to increased greenhouse-gas (GHG) concentrations, the predominant global climate change forcing. Modeled responses to doubled CO<sub>2</sub>, or emission scenario projections at the end of the twenty-first century tend to suggest increases in mean monsoon rainfall ([Turner and Annamalai 2012](#); [Ueda et al. 2006](#); [Cherchi et al. 2011](#); [Kitoh et al. 2013](#)). However, a decreasing trend of Indian summer monsoon rainfall (ISMR) has been found in multimodel ensemble (MME) mean assessments of phase 5 of the Coupled Model Intercomparison Project (CMIP5) ([Guo et al. 2015](#)). By comparing CMIP5 historical experiments with those containing only a single varying forcing experiment (aerosol only and GHG only), [Guo et al. \(2015\)](#) attributed the decreasing trend of the ISMR since the 1950s to aerosol, while, when only GHG forcing is used, rainfall increased. This result for India is also captured at the hemispheric scale: [Kitoh et al. \(2013\)](#) demonstrated MME mean decreases in Northern Hemisphere (NH) monsoon rainfall over the twentieth century in historical integrations. Further, [Polson et al. \(2014\)](#) used a subset of CMIP5 historical single-forcing experiments to attribute the reduced NH monsoon precipitation to increased

aerosol emissions, relating to a reduced temperature contrast between the NH and Southern Hemisphere (SH). This suggests that the impact of nonlocal aerosols on the monsoon may also be important.

By grouping CMIP5 models depending on their inclusion of parameterizations of aerosol indirect effects, [Guo et al. \(2015\)](#) were further able to show that the indirect effect of aerosol on cloud was key to producing a decreasing rainfall trend. This also explained why CMIP3 models did not simulate a decrease in rainfall, since these models rarely incorporated indirect effects ([Fan et al. 2010](#)).

The main anthropogenic aerosols over India are sulfate and carbonaceous aerosols. These aerosols modify planetary albedo by scattering and absorbing solar radiation ([Charlson et al. 1992](#)). But by interacting with clouds, thereby modifying cloud optical properties and cloud amount, these aerosols also modify cloud albedo ([Twomey 1977](#); [Albrecht 1989](#); [Ackerman et al. 2000](#); [Cook and Highwood 2004](#)). Though both aerosols reduce insolation at the surface, thereby having a negative radiative effect, sulfate scatters solar radiation back to space and thus also has a negative radiative effect at the top of the atmosphere (TOA); while carbonaceous aerosols, especially BC, absorb solar radiation, heat the atmosphere, and have a positive radiative effect at the TOA ([Forster et al. 2007](#)). These differing radiative characteristics of different aerosol species suggest that the ISMR may respond differently to changes in each type. Both sulfate and carbonaceous aerosol emissions have increased from India in the twentieth century. Comparing emissions over India using the representative concentration pathways (RCPs) database used to drive historical and future climate scenarios in CMIP5 ([Smith et al. 2001](#); [Bond et al. 2007](#); [Schultz et al. 2008](#)), sulfur dioxide emissions have increased tenfold from 0.78 kg m<sup>-2</sup> s<sup>-1</sup> in 1951 to 7.91 kg m<sup>-2</sup> s<sup>-1</sup> in 2000; BC emissions have more than doubled from 0.74 to 1.67 kg m<sup>-2</sup> s<sup>-1</sup>; and organic carbon has nearly tripled from 1.74 to 4.75 kg m<sup>-2</sup> s<sup>-1</sup> over the same period.

There is little doubt that increased concentrations of scattering aerosols can lead to reduced monsoon rainfall. For example, [Ramanathan et al. \(2005\)](#) suggested that aerosols had limited the surface warming over India related to GHG increases, reducing monsoon rainfall. Similarly, [Johns et al. \(2003\)](#) and [Ashrit et al. \(2003\)](#) used experiments of future GHG scenarios to show that monsoon rainfall increases relatively less when sulfate aerosol effects were included, compared to greenhouse gases alone.

The elevated heat pump (EHP) mechanism ([Lau et al. 2006](#); [Lau and Kim 2006](#)) is one of the proposed mechanisms by which absorbing aerosol can modulate monsoon

rainfall. Anomalous accumulation of dust and BC absorbing aerosol against the southern slopes of the Himalayas in the premonsoon period and the resultant absorption of shortwave radiation lead to an elevated heating anomaly that reinforces the large-scale meridional tropospheric temperature gradient and leads to intensification of the monsoon over the Indian subcontinent during June–July. The intensity of ISMR can be reduced during the later stages of the ISM, as a result of both aerosols washing out and the cooling of the surface temperature following increased cloudiness in the early ISM stage (Meehl et al. 2008). Besides, other studies (Bollasina et al. 2008; Nigam and Bollasina 2010) have argued that the semidirect effect of absorbing aerosols that reduces cloud cover and increases heating over the land surface during the premonsoon period can strengthen the Indian summer monsoon during June and July.

Though the ISMR is better represented in CMIP5 models than in CMIP3 models (Sperber et al. 2013), other authors point out that many GCMs still fail to reproduce rainfall trends over India, and the mechanisms involved are not well understood (Saha et al. 2014; Ramesh and Goswami 2014). With increasing GHG concentrations and global warming in the present day and projected into the future, modeling studies project an increase of ISMR (Turner and Annamalai 2012), though the monsoon circulation could be weakened (Ueda et al. 2006; Cherchi et al. 2011; Krishnan et al. 2013). However, others (Roxy et al. 2015) have argued that the observed decreasing trend of ISMR is actually caused by SST warming, itself due to greenhouse warming. Roxy et al. (2015) argue that forced ascent emanating from intense SST warming in the equatorial Indian Ocean leads to anomalous subsidence over India and reduced rainfall. There is still considerable diversity among the CMIP5 models as to which indirect effects are included and how they are parameterized (see, e.g., Wilcox et al. 2013; Ekman 2014) and in the driving emissions of these aerosols on which models rely. From simulations of the Aerosol Comparisons between Observations and Models (AeroCom) phase II hindcast experiment, Pan et al. (2015) found underestimations of aerosol loading over South Asia compared to satellite- and ground-based measurements.

The majority of studies have used global aerosol forcing or emissions to study monsoon rainfall change. At the hemispheric level, Shindell et al. (2012) have shown that, by confining forcings into separate latitudinal bands, the Indian monsoon responds differently to forcing from different latitudes and from different aerosol species. However, unlike well-mixed GHGs, the pattern of aerosol loading is inhomogeneous and strongly perturbed by precipitation and advection, and

therefore even these zonal-mean experiments are a simplification of the real forcing pattern. In particular, since anthropogenic aerosol emissions have increased dramatically since the 1950s over Asia, while they have decreased over western Europe and North America, it is still unclear how these regional aerosol changes may have altered ISMR. Bollasina et al. (2014) used the GFDL CM3 coupled model to explore local and nonlocal aerosol impacts on the South Asian monsoon. By keeping local or nonlocal anthropogenic aerosol emissions at 1860s levels while letting other anthropogenic and natural forcings evolve, they found that local aerosols dominate the South Asia rainfall decrease during the second half of the twentieth century, while remote aerosols strongly affect surface temperature and circulation. However, in their experiments, the nonlinearity between aerosols and other forcing agents may feature prominently in the overall response.

By answering the following three questions in this paper, we will help to improve understanding of the aerosol impact on long-term rainfall changes over India:

- What are the most important anthropogenic aerosol changes for ISMR?
- What is the relative impact of changing aerosols compared to changing GHGs and the observed SST warming on ISMR?
- What is the relative impact of local aerosol changes over India compared to aerosol changes elsewhere?

We will address the above questions using the Hadley Centre Global Environmental Model version 2 (HadGEM2) atmospheric GCM (AGCM) to perform a series of observation-based and sensitivity experiments. The remaining text is organized as follows: Section 2 introduces the model and experiments. Section 3 explores impacts of different types of aerosol on monsoon rainfall. In section 4, the importance of aerosol impacts on monsoon rainfall are compared to the effects of warming SST, much of the signal of which is a result of increasing GHG concentrations. The local aerosol impacts over India are compared with those forced from remote regions in section 5 before we offer our conclusions.

## 2. Model and experiments

### a. Model

The HadGEM2 is used in this study. HadGEM2 is the name of a model family that comprises a range of specific model configurations incorporating different levels of complexity but with a common physical framework (Martin et al. 2011). Several configurations from the HadGEM2 family participated in the CMIP5

multimodel experiment, but here we use its atmospheric component HadGEM2-A, which also includes modules for aerosol, land surface exchanges, hydrology, and river routing. The atmospheric component uses a horizontal resolution of  $1.25^\circ \times 1.875^\circ$  in latitude and longitude, respectively, with 38 layers in the vertical extending to over 39 km in height and with a model time step of 30 min (Collins et al. 2011).

The HadGEM2 aerosol module is the Coupled Large-Scale Aerosol Simulator for Studies in Climate (CLASSIC) (Bellouin et al. 2011). This aerosol module has the capability to contain numerical representation of up to eight tropospheric aerosol species (externally mixed): ammonium sulfate, mineral dust, sea salt, fossil-fuel BC, fossil-fuel organic carbon (OC), biomass burning aerosols, secondary organic aerosols, and ammonium nitrate aerosols. However, we have switched off the interactive mineral dust scheme in our experiments because of biases identified over the region of interest, as explained later. All species exert a direct radiative effect. In this aerosol module, all species except mineral dust and BC also exert first and second indirect effects. Our earlier study (Guo et al. 2015) has already demonstrated the importance of including indirect effects of aerosol (aerosol–cloud interactions) for accurate attribution of climate impacts over South Asia. Emissions or chemical production of mineral dust, sea salt, and nitrate aerosols are interactive (i.e., production is related to near-surface wind, humidity, etc.).

The interactive sulfur cycle of HadGEM2 is described by Jones et al. (2001) and Roberts and Jones (2004). The cycle starts with emissions of sulfur dioxide and dimethyl sulfide, which are oxidized into sulfates by dry oxidation with the hydroxyl radical and wet oxidation with ozone and the peroxide radical. Sulfate is represented by three prognostic tracers representing different sizes and properties; these are known as the Aitken and accumulation modes and a mode for sulfate dissolved in cloud droplets. Mass is exchanged between those modes by nucleation, evaporation and reevaporation, coagulation and merging, and diffusion (Bellouin et al. 2011). Sulfate is scattering aerosol; at 550-nm wavelength, single-scattering albedos are 1.0 for both Aitken and accumulation modes. As a type of hydrophilic aerosol, the optical properties change with humidity. For Aitken mode, the specific extinction coefficients at 550 nm are 0.001, 0.004, and  $1.1 \text{ m}^2 \text{ g}^{-1}$  at 0%, 60%, and 100% relative humidity. For accumulation mode, the specific extinction coefficients at 550 nm are 3.1, 5.8, and  $182.6 \text{ m}^2 \text{ g}^{-1}$ , respectively (Bellouin et al. 2011).

BC is represented by three prognostic tracers as fresh, aged, and in-cloud dissolved modes. The

single-scattering albedo for both fresh and aged mode BC is 0.41, and the specific extinction coefficient is  $5.4 \text{ m}^2 \text{ g}^{-1}$  at 550 nm.

Emissions for aerosol species or their precursors are prescribed as monthly data and are emitted from either the surface or an elevated level to represent emissions from chimney height. Figure 1 shows the change of sulfur dioxide and BC emissions from preindustrial to present day. Data are sourced from the RCPs database (Smith et al. 2001; Bond et al. 2007); these emissions are commonly used among all models in the CMIP5 database. For both aerosol species, emissions increase over western Europe, North America, and East and South Asia. For BC, emissions also increase over central Africa and South America. This difference in BC emissions arises as a result of not only fossil-fuel burning, but also biomass burning, which shows higher emissions during winter and spring over India. The RCP emissions are comparable to other emission inventories [e.g., the AeroCom phase II (A2) Aerosol Chemistry Climate Model Intercomparison Project (ACCMIP) (Diehl et al. 2012)]. The annual mean emissions in South Asia for the period of 2000–07 from the RCPs are  $8.02 \text{ Tg yr}^{-1}$  of sulfur dioxide and  $0.64 \text{ Tg yr}^{-1}$  of BC, which is very close to the values of  $7.46 \text{ Tg yr}^{-1}$  for sulfur dioxide and  $0.65 \text{ Tg yr}^{-1}$  for BC from A2-ACCMIP. After adding BC emissions from biomass burning, the annual mean BC emission in South Asia for the 2000–07 period is  $0.81 \text{ Tg yr}^{-1}$ .

Annual mean (1979–2005) aerosol optical depths (AODs) at 550 nm for sulfate aerosol in the Sulp experiment and for BC aerosol in the BC and BC $\times$ 5 experiments over India are shown in Figs. 2a–c. The spatial patterns of AOD are similar to those in emissions: that is, the highest AOD is located over the IGP. For further more detailed comparison, the annual cycles of simulated AODs over (the nearest gridpoint to) Kanpur ( $26.51^\circ\text{N}$ ,  $81.23^\circ\text{E}$ ) are compared with AERONET observations in 2004 (Fig. 2d). Sulfate AOD shows a single peak during the summer monsoon season [June–September (JJAS)]. This is due to the emissions and because sulfate aerosol is hygroscopic such that sulfate AOD increases with relative humidity; it is also due to the increase of solar radiation during summer when the solar zenith angle decreases. The BC AOD features an opposite cycle, being higher during winter and spring because of higher emissions from biomass at that time. In general, HadGEM2-A captures the spatial distribution and seasonal cycle of aerosol forcings over India. However, since we include only one aerosol species at a time, the magnitudes of forcing are smaller compared to observations and simulations using multiple aerosol species (Pan et al. 2015).

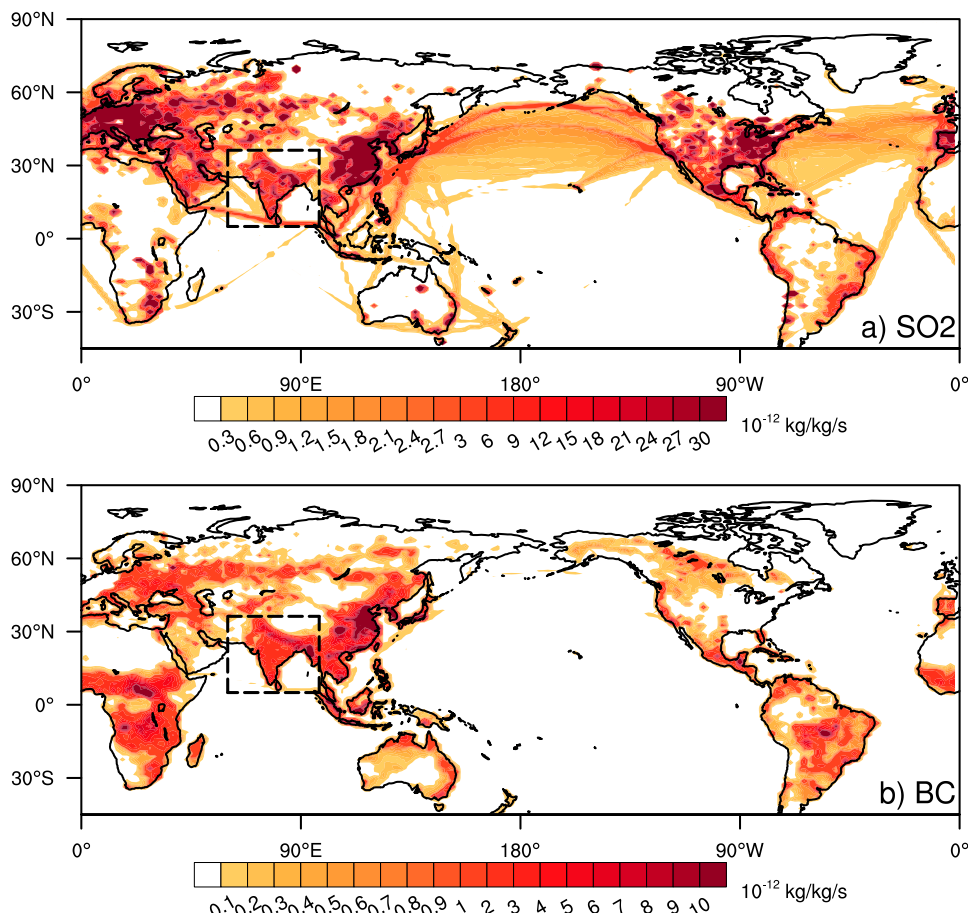


FIG. 1. Change of emissions ( $10^{-12} \text{ kg kg}^{-1} \text{ s}^{-1}$ ) from the preindustrial (1860) to present-day (1976–2005) periods: (a)  $\text{SO}_2$  and (b) BC. Data are from the RCPs database (Smith et al. 2001; Bond et al. 2007).

### b. Experimental design

We performed a series of experiments using HadGEM2-A as summarized in Table 1. Each of these experiments is integrated for 30 years and features six ensemble members, using initial condition perturbations, in order to enable verification of the statistical significance of results. The Control experiment is the benchmark with all aerosol forcings (including sulfate, BC, and OC) set to year 1860 values and thus approximately represents preindustrial conditions. The emissions of aerosols or their precursors are prescribed as a seasonal cycle; SSTs are varied monthly over the 1871–1900 period, derived from the AMIP forcing dataset defined by the Program for Climate and Model Diagnosis and Intercomparison (PCMDI) (Hurrell et al. 2008).

We briefly describe the behavior of the monsoon in the HadGEM family of models. Sperber et al. (2013) have examined the coupled version of the model, HadGEM2-ES, in an assessment of performance against

other CMIP5 GCMs for the Asian monsoon. CMIP5 models typically feature dry biases over India, of order  $5 \text{ mm day}^{-1}$  during JJAS, in association with a weak lower-tropospheric monsoon circulation. Sperber et al. (2013) show that the HadGEM2-ES model performs better than average at representing the spatial pattern of Asian monsoon precipitation and winds compared to other CMIP5 models. Levine and Turner (2012) have shown that the atmosphere-only version of the model features more precipitation than the coupled version. We will discuss later the possible impact of the model dry bias on the response to changing aerosol forcing.

#### 1) SINGLE AEROSOL SPECIES EXPERIMENTS

To explore the impact of single aerosol species, in the Sulp experiment, we perturb the global anthropogenic emissions of sulfur dioxide to their present-day levels (1976–2005), while other forcings remain at 1860 values. Similarly, present-day BC emissions are used in our BC experiment. Since BC and organic carbon have different

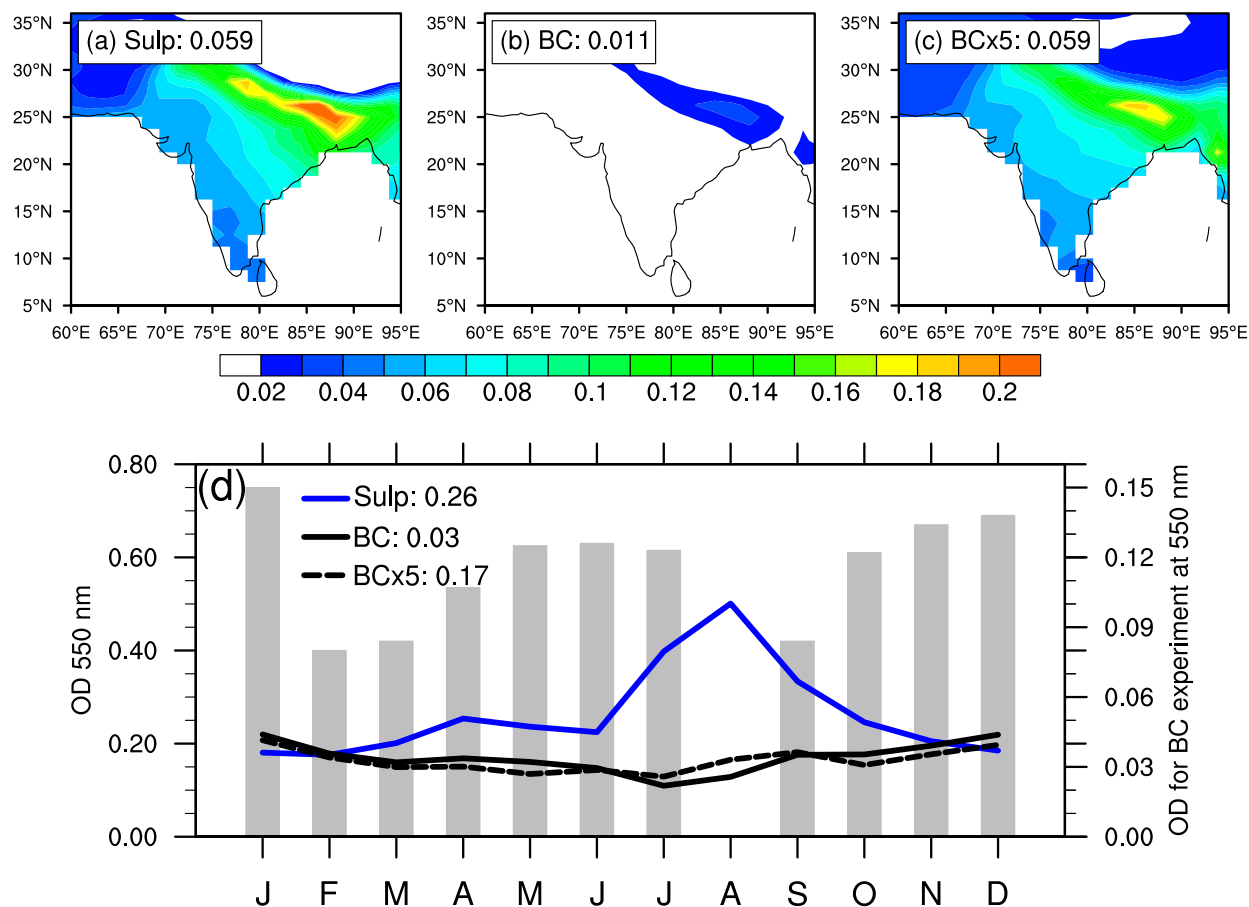


FIG. 2. Annual mean (1976–2005) AOD at 550 nm over India for (a) sulfate aerosol in Sulp experiment and for BC aerosol in (b) BC and (c) BC $\times$ 5 experiments. The area-averaged values are also shown in the top-left labels within each panel. (d) Monthly AOD at 550 nm over Kanpur (26.51°N, 81.23°E) during 2004 for sulfate AOD in the Sulp experiment (blue solid line) and BC AOD in the BC experiment (black solid line) and BC $\times$ 5 experiment (black dashed line). Annual mean values are also listed in the legend alongside the names of each experiment. Gray bars show the total AERONET AOD over Kanpur during 2004 [data are from Pan et al. (2015)]. Note that a different scale is used for BC experiments.

spectral characteristics and are coemitted in reality, we shall also test their combined impact in the Carbon experiment, in which we force with present-day BC and organic carbon emissions. In each case, monthly varying AMIP SSTs over the 1871–1900 period are used as the lower boundary forcing. We complete our global single-forcing aerosol experiments with Sulp\_DI, in which we switch off the indirect effects of aerosol in order to consider only direct radiative effects, and BC $\times$ 5, in which global BC emissions have been scaled up by 5 times their present-day values. We perform BC $\times$ 5 since we anticipate the result of BC forcing to be small.

Dust is another important aerosol affecting ISMR for the reasons mentioned in Lau et al. (2006), Vinoj et al. (2014), Lau (2014), Kim et al. (2015), and D'Errico et al. (2015). However, lengthy discussion of dust aerosol is beyond the scope of this study. This is partly because we

focus on anthropogenic aerosols and how the observed increasing trends in their emissions contribute to variations in ISMR. It is difficult to directly observe trends in dust aerosol, as a natural aerosol source. However, the aforementioned studies argued that, even without direct observations of dust emissions trends, the impact of dust aerosol on the monsoon could still be altered by changing dynamical feedbacks induced by other forcings, such as greenhouse gases or, in the case of this study, anthropogenic aerosols. However, we acknowledge that there are large uncertainties in dust simulation in HadGEM2. As shown in previous studies (e.g., Pan et al. 2015), dust AOD in HadGEM2 is much larger than in observations and other models over India. Were we to include the effects of dust, this dust bias could mask out impacts from other aerosols. Considering the important role that dust plays in changing ISMR, especially via the EHP

TABLE 1. Experiments performed and external forcings prescribed in each experiment. PD uses monthly varying emissions or concentrations forcing from January 1976 to December 2005; PI indicates forcing is set to year 1860, except for SSTs, which are monthly varying SSTs from January 1871 to December 1900. Each experiment is run for 30 years and has six ensemble members.

Experiment	Aerosol			SST and sea ice
	Sulfate	Black carbon	Organic carbon	
Control	PI	PI	PI	PI
Sulp	PD	PI	PI	PI
Sulp_DI <sup>a</sup>	PD	PI	PI	PI
Sulp_India	PD (within India) <sup>b</sup>	PI	PI	PI
Sulp_RW	PD (outside India)	PI	PI	PI
Carbon	PI	PD	PD	PI
BC	PI	PD	PI	PI
BC×5	PI	PD(×5)	PI	PI
BC×5_India	PI	PD×5 (within India)	PI	PI
BC×5_RW	PI	PD×5 (outside India)	PI	PI
SST <sub>obs</sub>	PI	PI	PI	PD
SST <sub>GHG</sub>	PI	PI	PI	PD <sup>c</sup>

<sup>a</sup> Sulfate emissions as in the Sulp experiment, but only the direct effect is included.

<sup>b</sup> The domain of India is defined as 5.0°–36.25°N, 60.0°–97.50°E.

<sup>c</sup> The PD SST for the SST<sub>GHG</sub> experiment is taken from GHG-only single-forcing runs of the coupled HadGEM2-ES model, as found in the CMIP5 database.

mechanism, in the following sections the results of the BC experiments will be explained with additional reference to the absence of dust aerosol in our experimental design.

We note that, by nature of their design, these single-forcing experiments performed in an atmosphere-only GCM will not include long-term oceanic adjustments to the aerosol forcing (Ganguly et al. 2012). Those effects would be included in experiments to be described in the following section, in which the observed changes in SST are applied to the model.

## 2) SST, GREENHOUSE GAS, AND AEROSOL FORCING

There is uncertainty in trends of monsoon rainfall over the late-twentieth century (Bollasina et al. 2011), and there are several potential drivers of change, the main one being greenhouse gases and aerosols. The bulk of the response to greenhouse gases manifests as surface temperature change, particularly in tropical SST. Thus, in addition, we explore the relative impact of aerosol and SST over the historical period. We perform an experiment forced by the change in monthly SST and sea ice as observed between the preindustrial period and 1976–2005 (SST<sub>obs</sub>). The observational SST and sea ice are AMIP data obtained from the PCMDI (Hurrell et al. 2008) and include the response to aerosols. In addition, we perform an experiment using the change in SST taken from the GHGs single-forcing experiment of the coupled HadGEM2-ES, which is archived in CMIP5 (SST<sub>GHG</sub>).

## 3) LOCAL AND REMOTE AEROSOL FORCING

To explore the relative impact of local aerosol emissions over India and aerosol elsewhere, a pair of

experiments with sulfur dioxide emission over India (5.0°–36.25°N, 60.0°–97.5°E) and outside India are performed (labeled Sulp\_India and Sulp\_RW, respectively). Similarly, a pair of experiments forced with enhanced BC emissions over India and outside India are performed (BC×5\_India and BC×5\_RW, respectively). The differences of aerosol emissions between the present day (PD) and preindustrial (PI) and the domain used for separating the local and remote experiments are illustrated in Fig. 1.

The next sections describe the results of these three experiment sets; results show the ensemble mean calculated from the six members of each experiment. A two-tailed Student's *t* test has been applied to test the robustness of differences between each of the experiments and the Control.

## 3. Determining the dominant aerosol species forcing in the South Asian monsoon

We describe here the results of the single-forcing experiments and mechanisms explaining the monsoon rainfall change. Figures 3a–c show the summer (JJAS) rainfall change when aerosol forcing is imposed from an individual species: Sulp, Carbon, and BC, respectively. The change is calculated by subtracting the Control from each aerosol forcing experiment. In Sulp (Fig. 3a), as sulfur dioxide emissions increase, rainfall reduces over the Indian subcontinent and East Asia and increases over the ocean. Continental rainfall decreases are statistically significant over the tropical Northern Hemisphere monsoon regions: India, East Asia, West

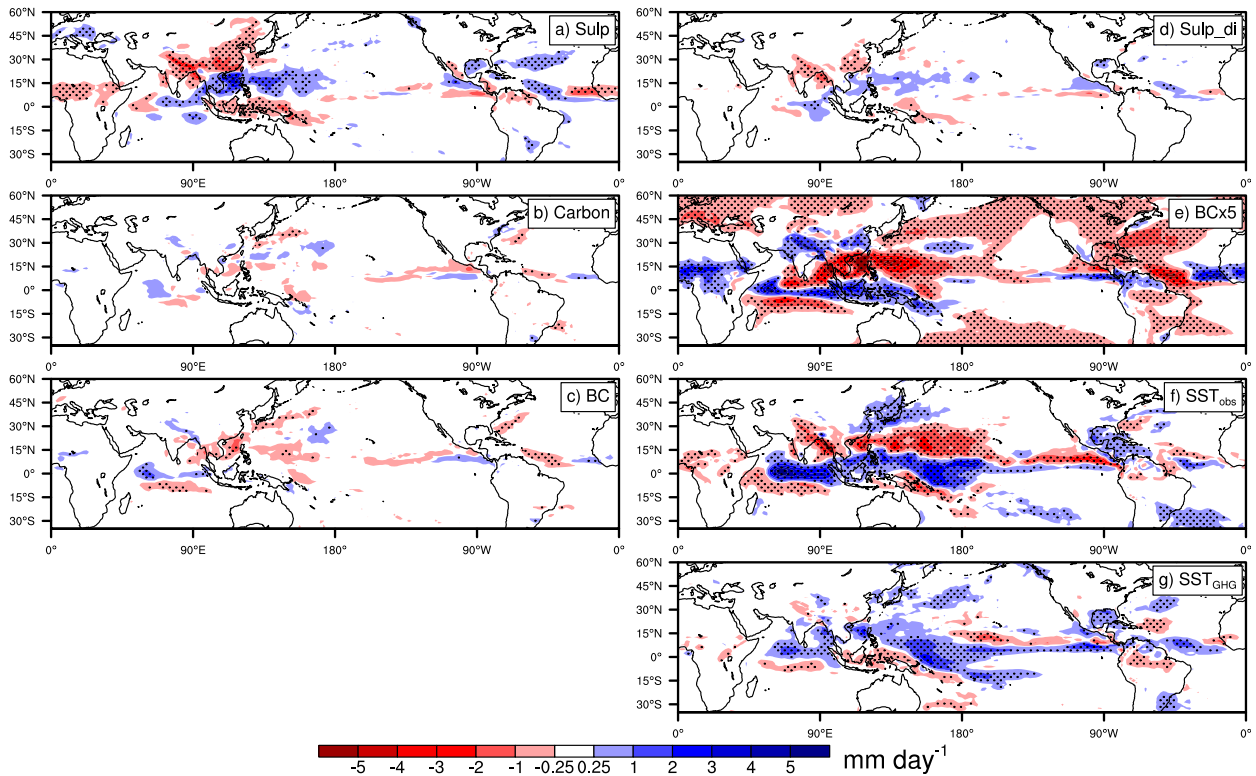


FIG. 3. JJAS rainfall changes ( $\text{mm day}^{-1}$ ) from the Control to the other experiments: (a) Sulp, (b) Carbon, (c) BC, (d) Sulp\_DI, (e) BC $\times$ 5, (f) SST<sub>obs</sub>, and (g) SST<sub>GHG</sub>. Results are averaged over the 30-yr integration in each case and across six ensemble members. Changes exceeding the 90% significance level using a Student's *t* test are stippled.

Africa, and the western coast of North America. Oceanic rainfall increases are significant over the tropics, especially south of the monsoon regions. Over the Indian region, the largest reductions in rainfall are over the IGP and Bay of Bengal (BoB). These results are consistent with earlier sensitivity tests and detection and attribution experiments implicating sulfates in declining ISMR (Guo et al. 2015; Polson et al. 2014).

Rainfall changes in Carbon and BC (Figs. 3b,c) are much smaller. Over India, the only statistically significant change due to carbonaceous aerosol or BC is a small increase of up to  $1 \text{ mm day}^{-1}$  over the IGP and along the foothills of the Himalayas. Because of the similarities between Carbon and BC experiments in rainfall change and surface temperature change, it can be concluded that the OC forcing is small. Therefore, we do not perform further experiments or analysis on the OC forcing. This small forcing of OC may be due to its combined scattering and absorbing optical properties or due to its low rate of emission compared to sulfate.

We now turn to local and large-scale temperature changes that may be leading to these changes in monsoon rainfall. Comparing surface temperature change in the Sulp, Carbon, and BC experiments (Figs. 4a–c),

differences in the large-scale meridional surface temperature contrast are consistent with the changes in rainfall. In the Sulp experiment (Fig. 4a), a hemispheric-scale continental surface temperature cooling appears over the NH, consistent with the net negative radiation change at the surface associated with large sulfate emissions there. In the Carbon and BC experiments, the surface temperature change in NH continents is not as homogeneous as in Sulp but instead is located over the midlatitudes, particularly in central-to-East Asia and the United States, and it is a positive change with a smaller magnitude. It is worth noticing the surface temperature response over India: the surface temperature increases with decreasing rainfall (Fig. 4a) but decreases (though insignificantly) with increasing rainfall (Figs. 4b,c), such that the change of surface temperature over India during the summer is opposite to its change elsewhere. A similar case is observed over tropical western Africa. This shows that local surface temperature change is responding to, rather than the reason for, the rainfall change. We remind the reader that the Indian monsoon is a more complex system than the simple local land–sea contrast from India to the Arabian Sea: it is the temperature gradient over a much larger scale, and

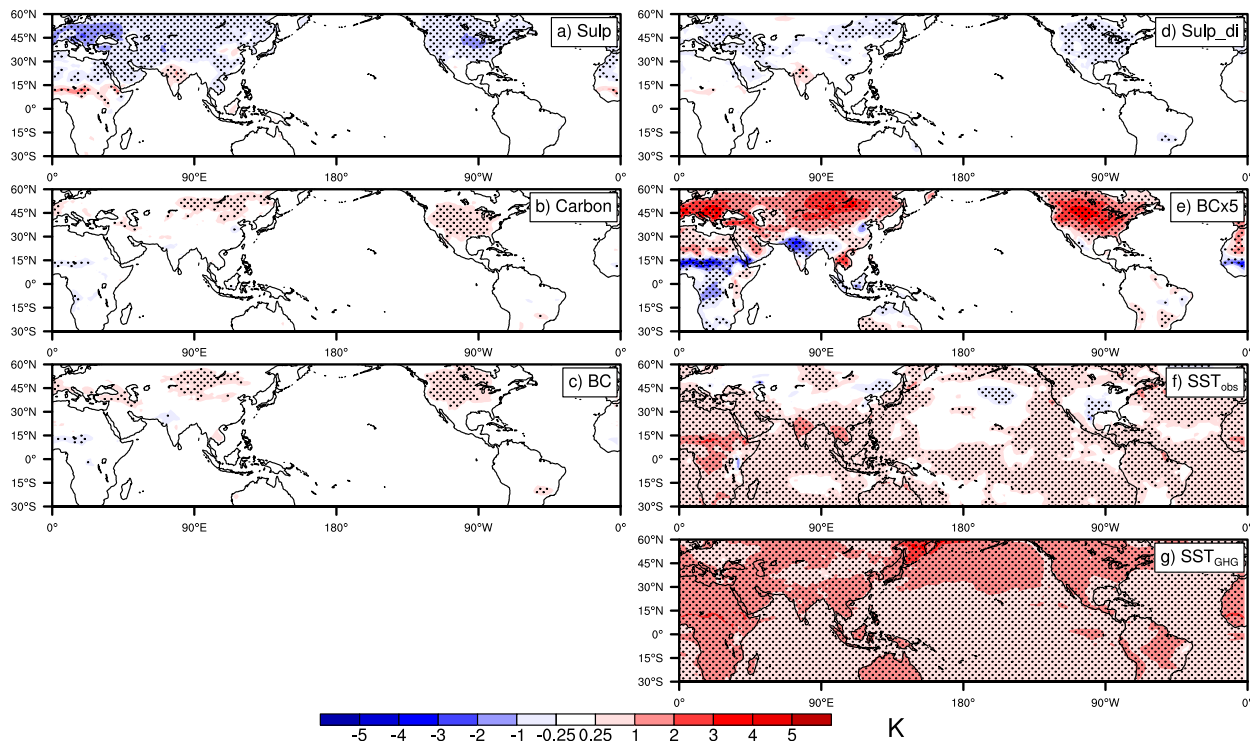


FIG. 4. Near-surface temperature changes (K) from the Control to the other experiments: (a) Sulp, (b) Carbon, (c) BC, (d) Sulp\_DI, (e) BC $\times$ 5, (f) SST<sub>obs</sub>, and (g) SST<sub>GHG</sub>. Results are averaged over the 30-yr integration in each case and across six ensemble members. Changes exceeding the 90% significance level using a Student's  $t$  test are stippled.

extending deep into the troposphere, that matters (Xavier et al. 2007).

Since our earlier work highlighted the importance of indirect aerosol effects (Guo et al. 2015), we now consider the Sulp\_DI experiment. When only the direct effect is considered for sulfate, the magnitudes of rainfall and surface temperature change are smaller (Figs. 3d and 4d). By analyzing the CMIP5 archive of historical experiments, Guo et al. (2015) pointed out that models including both direct and indirect effects have a larger decrease in rainfall over India and produce the observed trend more faithfully. The result here is consistent with that analysis. As we shall see later, the rainfall response to sulfate includes components from both the locally emitted aerosol and remote sources.

As described above for the BC experiment, the impact of BC on ISMR is limited, and the EHP mechanism cannot be detected. Therefore, we completed an additional experiment with a perturbation in emissions to 5 times the present-day levels of BC emissions (i.e., BC $\times$ 5). This shows a clear rainfall increase near the foothills of the Himalayas (Fig. 3e) and a large homogeneous surface warming over NH land. This clearly demonstrates the positive net radiative impact of NH BC loading on the surface for these larger concentration

changes. To study the EHP mechanism (Lau et al. 2006) in more detail, Fig. 5 shows the monthly evolution of zonal-mean temperature profile and meridional overturning circulation at Indian longitudes over the pre-monsoon to monsoon onset period. In April, there is a positive temperature anomaly over the Himalayas. Over the southern slopes of the Himalayas (20°–30°N), in the lower atmosphere (850–600 hPa), the heating anomaly is accompanied with anomalous ascent. This is where heavy BC loading accumulates according to Lau et al. (2006), and the response of temperature and vertical motion is evidence that the EHP mechanism does exist in our model. With the onset of ISMR during late May and June, Fig. 5 shows BC intensifying the summer monsoon overturning circulation (and rainfall, as shown in Fig. 3e). However, once monsoon rainfall prevails over the whole country during July, BC is removed from the mid-to-lower troposphere by rain (see Fig. S1), and its impact on monsoon circulation is not as strong in July as in May and June. This is consistent with the model experiments of Meehl et al. (2008).

Thus, with enhanced BC concentrations, the EHP mechanism does exist and enhances monsoon rainfall during the monsoon season. However, a certain intensity of BC forcing is needed to make this mechanism

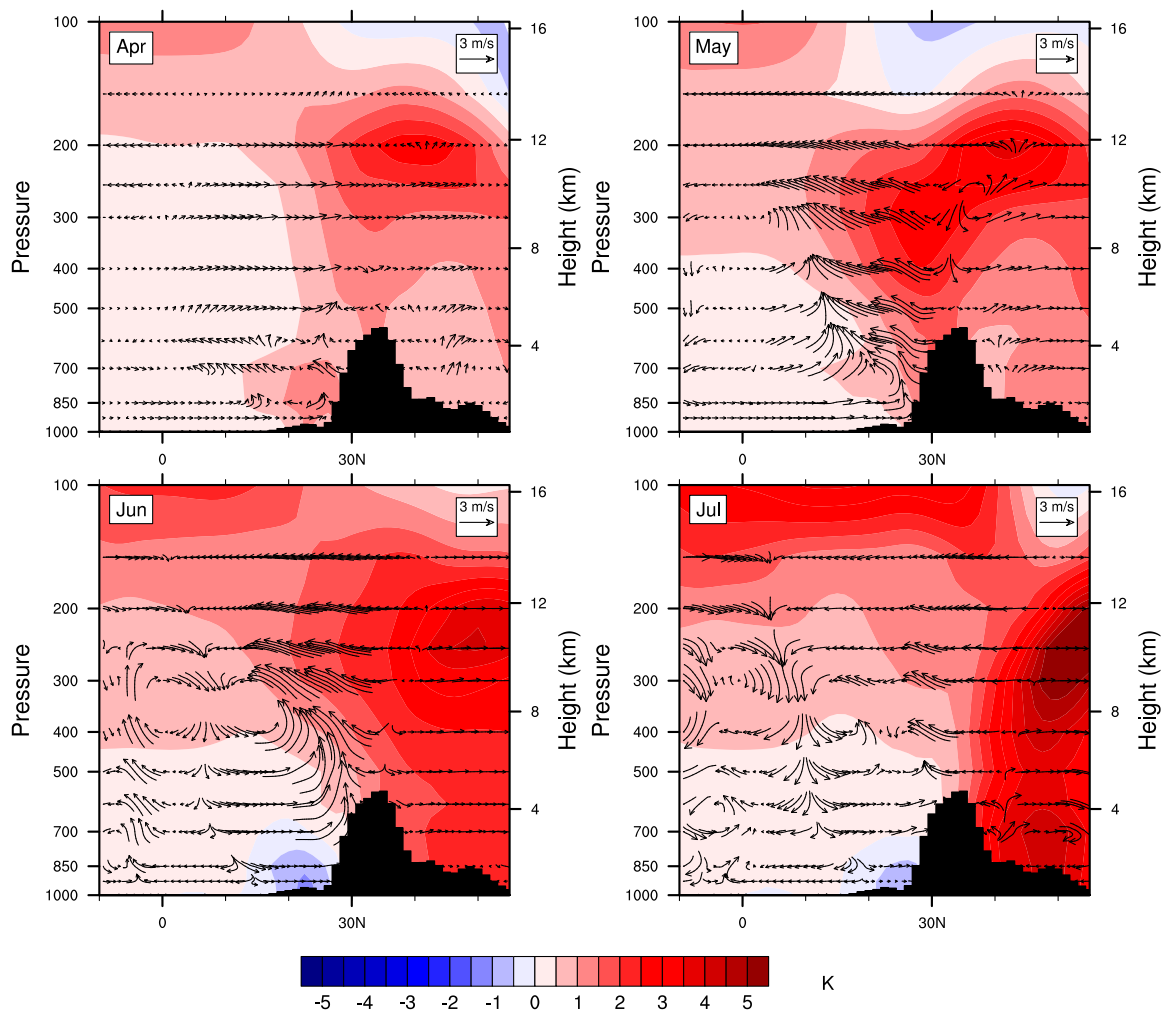


FIG. 5. Monthly zonal-mean (averaged over  $70^{\circ}$ – $100^{\circ}$ E) change of atmospheric temperature (shaded; K) and meridional circulation (vector;  $\text{m s}^{-1}$ ) for the BC $\times$ 5 experiment minus Control. Vertical velocity is multiplied by 200.

stand out from atmospheric internal variability and other competing forcings. Since both external forcings and atmospheric internal variability have a wide range of uncertainties among different models, it is understandable why the detection of the EHP mechanism has been ambiguous from previous studies. While our BC $\times$ 5 experiment could be regarded as a sensitivity test, there is evidence to suggest that current BC loadings over South Asia are underestimated: a recent study by Pan et al. (2015) reported a 60%–90% underestimation of winter BC surface concentrations in models compared to observations in six stations over India. As we shall see later, however, it is also worth remembering that it is not just the local BC emissions that yield a response in ISMR.

By comparing the impacts of different aerosol species in this section, we have shown that historical forcing

from sulfate aerosols is dominant on the monsoon compared to BC in this model. The EHP mechanism is undetectable in the HadGEM2 model unless BC emissions are scaled up. In the next section, we will discuss the relative impact of the dominant aerosol emission (sulfates) and SST warming on the monsoon.

#### 4. The relative impacts of sulfate forcing and SST warming

The Indian monsoon is known to respond to other forcing agents: for example, greenhouse gases such as carbon dioxide (Ueda et al. 2006; Cherchi et al. 2011; Roxy et al. 2015). Expected responses to warming are generally explained to relate to enhanced moisture convergence, arising from the warmer Indian Ocean [e.g., as reviewed in Turner and Annamalai (2012)]. However, while the

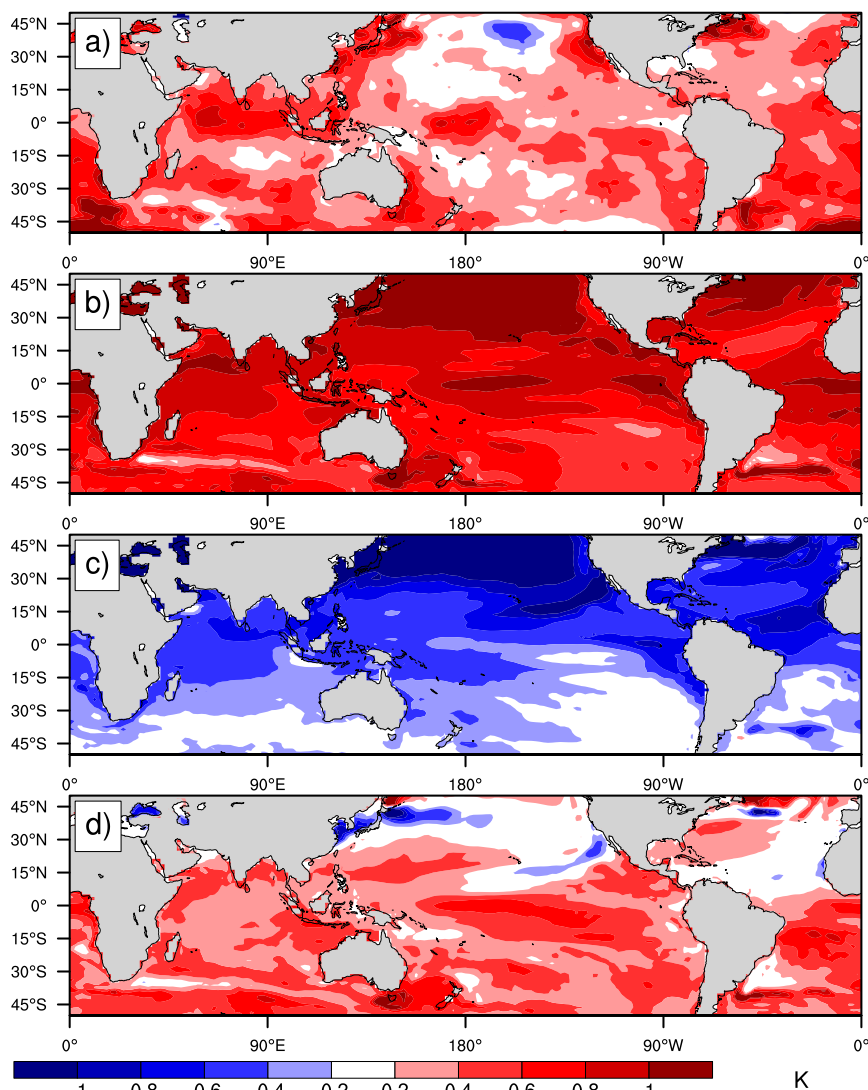


FIG. 6. Difference of annual mean SST (PD - PI) (K) of (a) AMIP SST from PCMDI (Hurrell et al. 2008); (b) derived from the coupled CMIP5 HadGEM2-ES historical experiment forced only by greenhouse gases; (c) derived from a HadGEM2-ES historical run forced only by aerosols; and (d) the sum of (b) and (c).

tropical SST warming due to increasing carbon dioxide concentrations in the atmosphere can increase rainfall in future projections (Ueda et al. 2006; Cherchi et al. 2011), our work above and in Guo et al. (2015) has suggested that declining rainfall over the twentieth century relates to increased aerosol emissions. Other authors (e.g., Roxy et al. 2015) claimed that the decreasing rainfall trend over the last century is largely due to SST warming caused by GHGs increasing. Therefore, the relative impacts of sulfate aerosol and SST warming need to be examined.

To compare the impacts of warming SST and increasing sulfate emissions on ISMR, the SST<sub>obs</sub> experiment with observational changes in SST is performed.

This, therefore, contains the SST changes in response to GHG, aerosol, and other forcings. We use observational SST (Fig. 6a) from the AMIP model forcing dataset, itself derived from HadISST data. As a comparison, SST changes between the preindustrial and present-day periods arising from greenhouse-gas forcing only and from aerosol forcing only are shown in Figs. 6b and 6c. These are from the single-forcing experiments in the coupled HadGEM2-ES model experiments submitted to CMIP5 and used in Guo et al. (2015). Under twentieth-century aerosol forcing, SST cools over NH midlatitudes (Fig. 6c), which corresponds to heavier NH continental emissions. Under GHG only, SSTs warm, with the

strongest signals (exceeding  $1^{\circ}\text{C}$ ) in the equatorial regions and in the extratropical North Pacific. As we sum up the SST changes due to sulfate and GHGs (Fig. 6d, which represents Fig. 6b + Fig. 6c), we see that SST cooling due to sulfate counteracts the warming due to greenhouse gases over NH midlatitudes, resulting in near-zero zonal-mean temperature change in the North Pacific midlatitudes of Fig. 6a. This results in the preferential SST warming over the tropics shown in observations (Fig. 6a). An important distinction with the hypothesis of Roxy et al. (2015), therefore, is that both GHG and aerosol have contributed to the pattern of observed SST change: aerosols reduce temperatures in NH midlatitudes and thus shift the thermal equator southward.

The rainfall change resulting from  $\text{SST}_{\text{obs}}$  is shown in Fig. 3f. Rainfall increases over the equatorial oceans, especially over the Indian Ocean and western Pacific, but decreases over adjacent continents, especially to the north over India and West Africa, amounting to a southward shift of the ITCZ and weakening of the NH monsoons. From a global point of view, rainfall responses to sulfate over land and to SST are similar over tropical monsoon areas, because of the weakening of the large-scale thermal contrast.

#### a. Meridional temperature gradient

To compare the change in large-scale meridional thermal contrast due to sulfate and SST in more detail, the seasonal cycles of the tropospheric temperature anomaly ( $\Delta\text{TT}$ ) are shown for the Control, Sulp, and  $\text{SST}_{\text{obs}}$  experiments (the black, blue, and red lines in Fig. 7, respectively). The tropospheric temperature (TT) is defined as the averaged atmospheric temperature between 200 and 600 hPa, and the  $\Delta\text{TT}$  is the difference of tropospheric temperature between a northern box ( $5^{\circ}\text{--}35^{\circ}\text{N}$ ,  $40^{\circ}\text{--}100^{\circ}\text{E}$ ) and a southern box ( $15^{\circ}\text{S--}5^{\circ}\text{N}$ ,  $40^{\circ}\text{--}100^{\circ}\text{E}$ ) [following Xavier et al. (2007), chosen to represent the meridional contrast]. The difference  $\Delta\text{TT}$  thus represents a large-scale heating gradient that drives the monsoon circulation. As Xavier et al. (2007) demonstrated, when  $\Delta\text{TT}$  changes sign from negative to positive, the onset of the monsoon rain occurs, while the monsoon withdraws when  $\Delta\text{TT}$  changes sign from positive to negative.

Figure 7a shows that both sulfate and SST produce a similar seasonal cycle of  $\Delta\text{TT}$ , in which the Indian summer monsoon features a later onset and earlier withdrawal compared to the control experiment. This is consistent with the rainfall reduction shown in Figs. 3a and 3f. When decomposing  $\Delta\text{TT}$  into its northern box (Fig. 7b) and southern box (Fig. 7c), different mechanisms causing monsoon rainfall reduction are revealed.

For sulfate, the weakening of  $\Delta\text{TT}$  is due to the cooling in the northern box, reflecting its location within Eurasia, where sulfate forcing is strong. For SST, tropospheric temperature increases in both the northern and southern boxes; however, a greater increase in the southern box reduces the gradient.

Following the results of section 3, it is also interesting to describe  $\Delta\text{TT}$  for the BC $\times$ 5 experiment (gray line in Fig. 7). The absorption of BC heats the troposphere over the northern box (Fig. 7b) and increases  $\Delta\text{TT}$ . Figure 7a shows that BC has a stronger influence during the premonsoon and monsoon onset period (April–June), but has less impact after July. If dust aerosol were included simultaneously with BC and externally coated by BC, as Lau et al. (2006) showed in their experiments, changes in ISMR could be observed as late as July. This is because, although local BC loading over IGP can be washed out, more absorbing dust aerosols are still being transported into the IGP region by the strengthened southwesterly monsoon flow (Lau et al. 2006; Vinoj et al. 2014; Kim et al. 2015; D'Errico et al. 2015).

#### b. Regional-scale changes

A closer look at the regional scale, however, shows more subtle differences in the impacts of sulfate and SST on ISMR. Figure 8 shows the seasonal cycles of two subregions of the Indian monsoon—BoB and IGP—for Control, Sulp,  $\text{SST}_{\text{obs}}$ , and  $\text{SST}_{\text{GHG}}$  experiments. Over BoB, the monsoon onset is delayed and monsoon rainfall is reduced in the  $\text{SST}_{\text{obs}}$  experiment; yet, in the Sulp experiment, neither monsoon onset nor seasonal monsoon rainfall differs from Control. In contrast, over the IGP, monsoon rainfall is noticeably reduced throughout the monsoon season in the Sulp experiment, but the change in the  $\text{SST}_{\text{obs}}$  experiment is small and only in June. Though patterns of rainfall change have a certain degree of similarity at the global scale, Fig. 8 shows that different mechanisms need to be considered on the regional scale for understanding the response of the monsoon to sulfate and SST changes.

Figures 9a and 9b show the change of zonal-mean meridional circulation and overturning streamfunction over India ( $75^{\circ}\text{--}100^{\circ}\text{E}$ ) during JJAS due to sulfate and observed SST. Both experiments show a slowing down of the summer monsoon meridional overturning circulation, but the reduction in the  $\text{SST}_{\text{obs}}$  experiment is larger. The outstanding feature in the  $\text{SST}_{\text{obs}}$  experiment is the anomalous ascending branch near the equator, which is a response to SST warming over the tropics, and it is not surprising for an AGCM to respond in this way when forced by preferential SST warming near the equator. In the Sulp experiment, there is no such anomalous equatorial ascent, and the outstanding

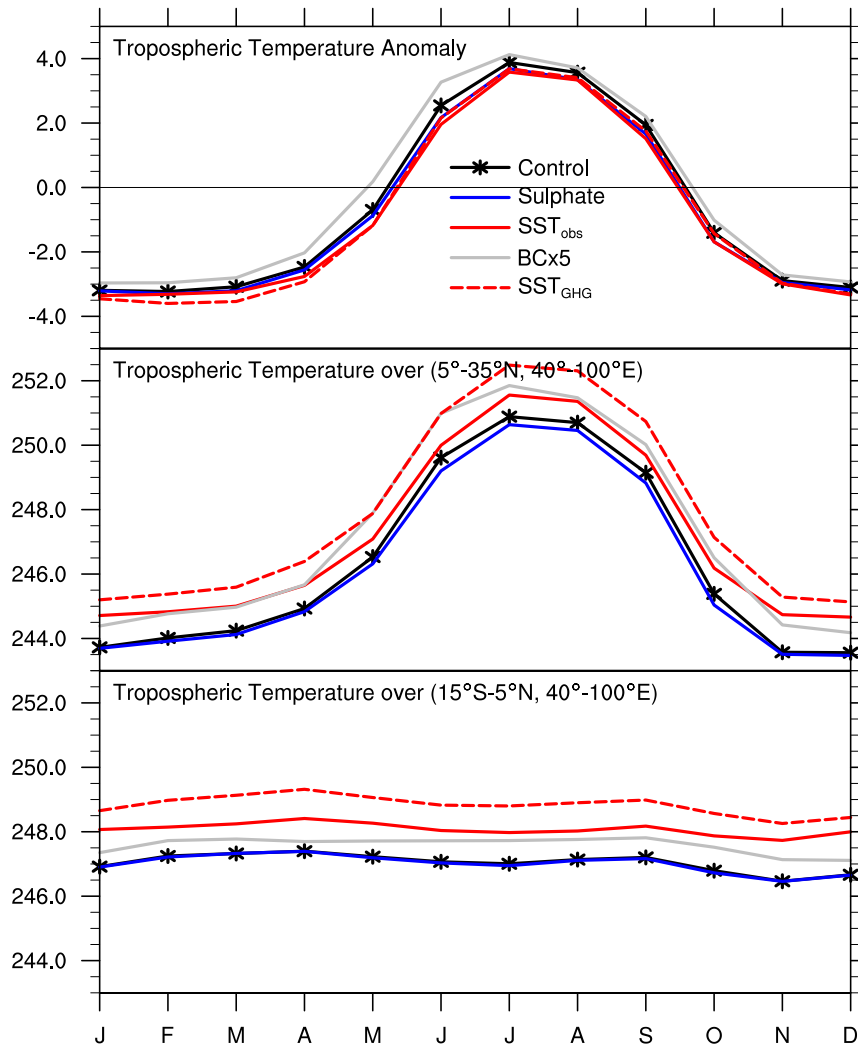


FIG. 7. Seasonal cycle of meridional tropospheric temperature gradient (K) after Xavier et al. (2007) calculated using (top) monthly data and its component regions: tropospheric temperature (K) over the (middle) northern box ( $5^{\circ}$ – $35^{\circ}$ N,  $40^{\circ}$ – $100^{\circ}$ E) and (bottom) southern box ( $15^{\circ}$ S– $5^{\circ}$ N,  $40^{\circ}$ – $100^{\circ}$ E).

feature is the descent near  $30^{\circ}$ N, which is consistent with the position of maximum sulfate loading (not shown).

Horizontally, the moisture flux and its divergence reveal more differences between the Sulp and  $SST_{obs}$  experiments (Figs. 9d,e). The moisture divergence change is large over the IGP in the Sulp experiment. In the  $SST_{obs}$  experiment, the same pattern is shown, but stronger, and with large changes in horizontal moisture divergence over the BoB and the western coast of India; there is also strongly enhanced convergence over the tropical Indian Ocean. Another difference between these two experiments is over East Asia. In the  $SST_{obs}$  experiment, there is an anticyclonic circulation change over the eastern coast of China, a sign of an intensified western North Pacific subtropical high (WNPSH). This

also aids weakening the mean westerly horizontal fluxes of moisture across India. Because the intensity and position of the WNPSH are key for positioning of the mei-yu front, the corresponding anomalous moisture convergence is shown from the Yangtze River delta extending northeastward to south Japan. However, in the Sulp experiment, anomalous moisture divergence covers the same region accompanied by a dry northerly moisture flux anomaly.

Although we have clearly shown that the observed SST change to the late-twentieth century is not simply the result of GHG-related warming, our results show that, when forced with this SST change, the monsoon weakens more strongly than when sulfate forcing alone over land is considered. This reflects the enhanced equatorial ascent

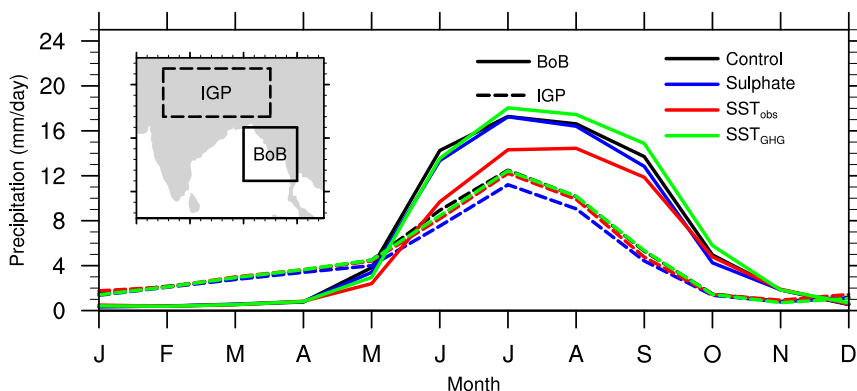


FIG. 8. Seasonal cycles of rainfall ( $\text{mm day}^{-1}$ ) averaged over the BoB (solid) and IGP (dashed) for four experiments: Control (black), Sulphate (blue),  $\text{SST}_{\text{obs}}$  (red), and  $\text{SST}_{\text{GHG}}$  (green). The inset map shows domains used for area average.

and resulting descent over India. It is clear though that SSTs alone do not represent the whole impact of GHG warming; our  $\text{SST}_{\text{obs}}$  experiment does not represent the whole, nor does the idealized equatorial Indian Ocean SST experiment of Roxy et al. (2015). In the absence of aerosol changes in the atmosphere, preferential NH SST

warming in the midlatitude Pacific Ocean and land surface warming over Eurasia due to the effects of enhanced carbon dioxide concentrations and vegetation feedbacks (Dong et al. 2009) would both act to strengthen the meridional thermal temperature contrast supporting enhancement of the South Asian monsoon.

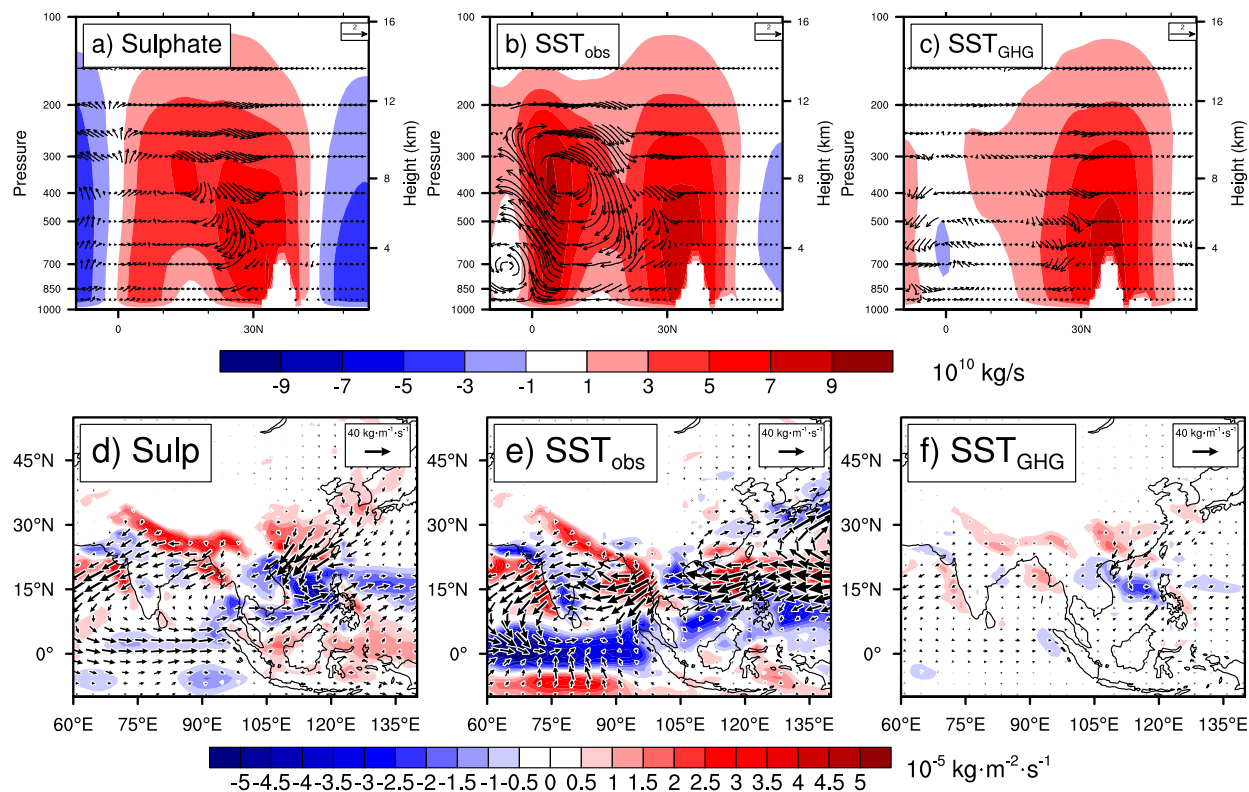


FIG. 9. JJAS changes (from preindustrial period) of zonal-mean meridional circulation (vector) and overturning streamfunction (shading) between  $75^{\circ}$  and  $100^{\circ}\text{E}$  for (a) Sulp and (b)  $\text{SST}_{\text{obs}}$  experiments. Units:  $10^{10} \text{ kg s}^{-1}$ ; vertical velocity is multiplied by 200. JJAS change of vertically integrated ( $1000\text{--}700 \text{ hPa}$ ) moisture flux (vector;  $\text{kg m}^{-1} \text{ s}^{-1}$ ) and moisture flux divergence (shading;  $\text{kg m}^{-2} \text{ s}^{-1}$ ) for (c) Sulp and (d)  $\text{SST}_{\text{obs}}$  experiments.

The impact of NH midlatitude SST warming is tested in the SST<sub>GHG</sub> experiment. The rainfall changes over the Indian Peninsula and BoB change sign (Fig. 3g), being no longer a decreasing trend but a weak increasing trend instead. The significant change occurs mainly over the BoB. As discussed above, rainfall change over the BoB is more sensitive to changes in SST, while, over the IGP, sulfate is dominant and rainfall change is not significant when forced with either the observed SST change or the SST change derived from the GHG single-forcing experiment. Figure 7a also shows the meridional tropospheric temperature gradient for SST<sub>GHG</sub>. It is similar to the SST<sub>obs</sub> experiment. Figures 9c and 9f show changes of the meridional Indian summer monsoon circulation and the moisture flux and the moisture flux divergence in the SST<sub>GHG</sub> experiment. Changes in the SST<sub>GHG</sub> experiment have much smaller magnitudes compared to the SST<sub>obs</sub> experiment. The similarity in the tropospheric temperature gradient (Fig. 7a) and the difference in the meridional monsoon circulation and moisture flux (Fig. 9) between SST<sub>GHG</sub> and SST<sub>obs</sub> indicate that rainfall over BoB is sensitive to an even larger temperature gradient than indicated by the Xavier et al. (2007) index.

It is also important to note that neither SST<sub>obs</sub> nor SST<sub>GHG</sub> experiments include the impact of increased GHG on land temperatures, since concentrations of GHG are left unchanged and important vegetation feedbacks will not alter the surface temperature. This may affect rainfall change since land surface temperature changes can alter the interhemispheric temperature gradient and thus the position of the ITCZ. The larger land fraction in the Northern Hemisphere means that the Northern Hemisphere warms disproportionately in response to GHG forcing compared to the Southern Hemisphere. However, as shown in previous studies that investigate trends of monsoon rainfall in atmosphere–ocean coupled simulations, including both GHG and aerosol forcings (Guo et al. 2015; Kitoh et al. 2013; Polson et al. 2014), aerosol is the main factor contributing to the observed downward trend of monsoon rainfall over land. This may be because aerosol forcing is currently outweighing the effect of GHG forcing over India. Additionally, this may also be due to monsoonal land rainfall responding less actively to the GHG forcing over land. For example, Fasullo (2012) noted that, although the land surface temperature increases under the GHG forcing, the lower-tropospheric relative humidity over land decreases at the same time. This could lead to a decrease in monsoon convection over land as a result of increased height of the lifting condensation level.

## 5. The relative impact of local and remote aerosol forcing on the South Asian monsoon

In the previous sections, we demonstrated that changes of ISMR possess features of the expected responses to changes in the large-scale temperature gradient as well as to regional features that are more dependent on the forcing mechanism. Since distributions of atmospheric aerosol are themselves inhomogeneous and have detailed regional footprints, the relative importance of global and regional aerosol changes is now discussed.

Figures 10a and 10b show JJAS rainfall changes due to imposing present-day local Indian sulfur dioxide emissions (Sulp\_India) and sulfur dioxide emissions outside India (Sulp\_RW). When local emissions only are used, the regions of significant rainfall change are also confined over the IGP along the foothills of the Himalayas (Fig. 10a). The area-mean rainfall change over this region in the Sulp\_India experiment is  $-0.28 \text{ mm day}^{-1}$ . With sulfate changes imposed elsewhere except for India (Fig. 10b), the pattern of change of rainfall is similar to the Sulp experiment (Fig. 3a); rainfall reduces over NH continents. The magnitude of rainfall reduction over India in Sulp\_RW, however, is weaker, at  $-0.75 \text{ mm day}^{-1}$ , and it is  $-0.88 \text{ mm day}^{-1}$  in the global Sulp experiment. This is likely due to the lack of local indirect effects over the IGP, where the Sulp\_RW experiment is lacking the high emissions of that region, as we showed in Fig. 1. Shindell et al. (2012) argued that the combined rainfall response to aerosol forcing from different regions can be linear. In their study, different regions are defined as zonal-mean latitudinal bands. They argued that the linearity can hold because of the small exchange of radiative agents and therefore radiative forcings on the latitudinal boundaries. Here, our sulfate experiments show that, when aerosol forcing is confined within an even smaller region within a boxed boundary, a similar linearity also holds approximately, with sulfate forcing within India contributing about a quarter of the rainfall decrease and sulfate forcing elsewhere contributing about three quarters.

The separation of local impact from remote impact is also performed for BC $\times$ 5, i.e., BC $\times$ 5\_India and BC $\times$ 5\_RW experiments. A difference compared to sulfate is that local BC emissions contribute very little to ISMR change (shown in Table 2). Instead, rainfall change during the monsoon is almost entirely due to large-scale changes in BC emissions. The rest-of-world changes in BC and sulfate emissions lead to the largest rainfall change over India. And this rainfall change is largely due to change in the large-scale temperature gradient change rather than the influence of remote aerosol emissions being transported to India.

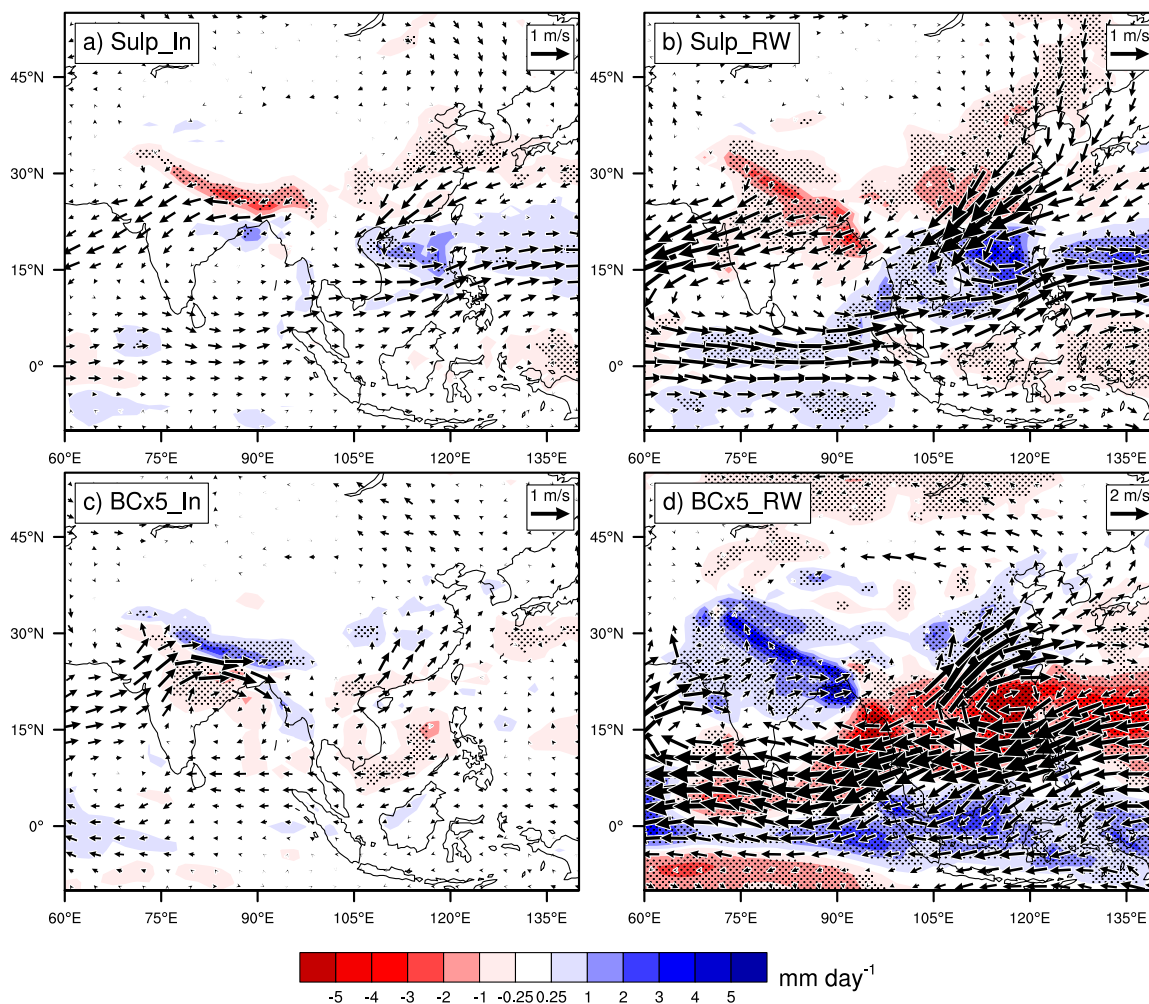


FIG. 10. JJAS changes (from preindustrial period) of rainfall (shading;  $\text{mm day}^{-1}$ ) and 850-hPa wind (vectors;  $\text{m s}^{-1}$ ) over Asia in (a) Sulp\_In, (b) Sulp\_RW, and (c) BCx5\_India, and (d) BCx5\_RW experiments. Rainfall changes exceeding the 90% significance level using a Student's  $t$  test are stippled.

At this point we can hypothesize on the impact of the dry monsoon rainfall bias in HadGEM2 (and prevalent in other CMIP5 models) on the results. In central India and outside of the IGP region, the dry bias may lead to a loading of aerosol that is too high, leading to a rainfall decrease that is too large in the case of local sulfate forcing, or an increase that is too large in the case of local BC. However, as Table 2 shows, the local aerosol forcing does not play the dominant role in the effects of anthropogenic aerosol on the monsoon. In the IGP region, rainfall in the model is strong, but, since the monsoon season is shorter at this latitude, biases will have lesser impact.

The remote impact of sulfate on ISMR is also manifested by its impact on the NH midlatitude SST. Compared to GHG forcing, the cooling effect of sulfate is exerted preferentially on the NH midlatitude ocean.

Therefore, the GHG-forced tropical SST warming becomes a prominent feature of the observed SST change. As shown in other studies (e.g., Roxy et al. 2015) as well as in section 4, the tropical SST warming is the main reason for reduced rainfall over BoB.

TABLE 2. JJAS changes of rainfall ( $\text{mm day}^{-1}$ ) averaged over northern India and its standard deviation ( $21^{\circ}$ – $35^{\circ}$ N,  $70^{\circ}$ – $90^{\circ}$ E) for experiments: Sulp, Sulp\_India, Sulp\_RW, BCx5, BCx5\_India, and BCx5\_RW. The standard deviation is calculated from six ensemble members for each experiment.

Aerosol	Emission Domain		
	Globe	India	RW <sup>a</sup>
Sulfate	$-0.88 \pm 0.22$	$-0.28 \pm 0.06$	$-0.73 \pm 0.20$
BCx5	$1.27 \pm 0.22$	$0.05 \pm 0.13$	$1.28 \pm 0.18$

<sup>a</sup> Emissions from the rest of the world, outside India.

## 6. Conclusions

Using HadGEM2-A, we investigated impacts of different anthropogenic aerosols on ISMR. We also compared the impacts of anthropogenic aerosols in the atmosphere and over land with impacts of SST changes, which include observed SST change due to GHGs and aerosols and SST change only due to GHG forcing. Finally, we discussed the relative importance of local and remote aerosol emissions on the monsoon.

Sulfate has a stronger impact on ISMR compared to carbonaceous aerosols, causing a rainfall decrease, especially over the IGP. Carbonaceous aerosols exert a smaller change on monsoon rainfall. But by exaggerating the growth in BC emissions by 5 times in a sensitivity test, rainfall increases, especially over northern India. We demonstrate that the EHP mechanism enhances convection during the premonsoon season and brings forward the monsoon onset.

We have shown that increases in sulfate forcing and SST warming dominated by a signal in the deep tropics cause ISMR to reduce. At the large scale, patterns of Indian rainfall change are similar and are attributable to the weakening of the large-scale meridional tropospheric temperature gradient. At the regional scale, impacts from sulfate and SST are different: the strongest rainfall reductions due to the SST are located over the BoB as a result of compensating descent responding to enhanced convection over the tropical Indian Ocean. Reduced monsoon rainfall due to sulfates is centered over the IGP as a result of the strong aerosol loading there and also indirect effects of aerosol on monsoon cloud. Both sulfate and SST weaken the monsoon circulation and shorten the summer monsoon season by delaying the onset and advancing the withdrawal. However, examination of the tropospheric temperature gradient anomaly reveals that the weakening in the SST<sub>obs</sub> experiment is due to heating over the central and southern Indian Ocean, but it is due to cooling over the NH continents in the Sulp experiment. With the SST<sub>GHG</sub> experiment that uses SST changes derived from a GHG single-forcing coupled experiment, the different mechanisms of impact of sulfate and GHGs on regional-scale rainfall change remain. Sulfate remains as the main factor contributing to rainfall decrease over the IGP, and the SST change due to GHGs forcing is the dominant factor that decides rainfall change over BoB. However, with the NH midlatitude SST warming playing a role in the SST<sub>GHG</sub> experiment, the rainfall trend over BoB changes from negative to positive.

Our results show that, with enhanced BC emissions, ISMR increases. The EHP mechanism does exist in HadGEM2-A (in the BC $\times$ 5 experiment, when present-day emissions are scaled up), and it advances the onset

of the monsoon; the EHP has a reducing impact as the season progresses, since the advancing monsoon reaches northern India in July. Despite our experimental design scaling up the BC emissions to show the EHP at work, there is evidence to suggest that BC aerosol loadings generated among the CMIP5 models are too low over northern India (Pan et al. 2015), so in some sense our sensitivity experiment can be justified.

The inhomogeneous distribution of aerosol emissions, with a particularly strong upward trend over northern India, suggests that local aerosol forcing could be as important as remote forcing to ISMR change. By separating local sulfate forcing (Sulp\_India) from the rest of the world (Sulp\_RW), we have shown that both local and remote sulfate contribute to rainfall reductions over India, especially over the IGP. The linear combination of rainfall reduction from Sulp\_India and Sulp\_RW is approximately comparable to rainfall decrease in Sulp, with local sulfate contributing a quarter of the reduction and remote sulfate contributing the rest. However, the same approximate linearity does not apply to BC. Though there is a narrow band of increased rainfall over the foothills of the Himalayas in BC $\times$ 5\_India, over a box-average South Asia region increases in the monsoon rainfall are largely due to BC forcing from the rest of the Northern Hemisphere. We also note the different conclusion to that drawn by Bollasina et al. (2014): they suggested the local aerosol is the predominant factor that changes rainfall over India/South Asia. One possible reason for this difference is that potential nonlinear feedbacks between aerosols and other forcing agents are featured in their experiments but are limited here since we fixed other forcing agents at 1860 levels. Another possible reason may be because of the forcing of dust aerosol. Therefore, to test how important these nonlinear feedbacks between aerosols and other forcing agents, or between different aerosol species, are, one could consider removing aerosol species one at a time to retain the nonlinearity. Besides, the effect of different biases between the two models cannot be ruled out.

The cooling effect of sulfate over the NH midlatitude ocean also remotely affects the ISMR. Though its impact on IGP is small, it is the main reason that reduces rainfall in the BoB. This highlights the danger of using SST-forcing experiments as simplifications in order to understand atmospheric responses to complex drivers, such as GHGs and aerosol emissions.

*Acknowledgments.* L. Guo, A. G. Turner, and E. J. Highwood are funded under the NERC Changing Water Cycle (South Asia) project SAPRISE (NE/I022469/1); A. G. Turner was funded by an NERC Fellowship (NE/H015655/1) for a portion of this work.

## REFERENCES

- Ackerman, A. S., O. B. Toon, D. E. Stevens, A. J. Heymsfield, V. Ramanathan, and E. J. Welton, 2000: Reduction of tropical cloudiness by soot. *Science*, **288**, 1042–1047, doi:10.1126/science.288.5468.1042.
- Albrecht, B. A., 1989: Aerosols, cloud microphysics, and fractional cloudiness. *Science*, **245**, 1227–1230, doi:10.1126/science.245.4923.1227.
- Ashrit, R., H. Douville, and K. Kumar, 2003: Response of the Indian Monsoon and ENSO–monsoon teleconnection to enhanced greenhouse effect in the CNRM coupled model. *J. Meteor. Soc. Japan*, **81**, 779–803, doi:10.2151/jmsj.81.779.
- Babu, S. S., and Coauthors, 2013: Trends in aerosol optical depth over Indian region: Potential causes and impact indicators. *J. Geophys. Res. Atmos.*, **118**, 11 794–11 806, doi:10.1002/2013JD020507.
- Bellouin, N., J. Rae, A. Jones, C. Johnson, J. Haywood, and O. Boucher, 2011: Aerosol forcing in the Climate Model Intercomparison Project (CMIP5) simulations by HadGEM2-ES and the role of ammonium nitrate. *J. Geophys. Res.*, **116**, D20206, doi:10.1029/2011JD016074.
- Bollasina, M., S. Nigam, and K.-M. Lau, 2008: Absorbing aerosols and summer monsoon evolution over South Asia: An observational portrayal. *J. Climate*, **21**, 3221–3239, doi:10.1175/2007JCL12094.1.
- , Y. Ming, and V. Ramaswamy, 2011: Anthropogenic aerosols and the weakening of the South Asian summer monsoon. *Science*, **334**, 502–505, doi:10.1126/science.1204994.
- , —, —, M. D. Schwarzkopf, and V. Naik, 2014: Contribution of local and remote anthropogenic aerosols to the twentieth century weakening of the South Asian Monsoon. *Geophys. Res. Lett.*, **41**, 680–687, doi:10.1002/2013GL058183.
- Bond, T. C., E. Bhardwaj, R. Dong, R. Jogani, S. Jung, C. Roden, D. G. Streets, and N. M. Trautmann, 2007: Historical emissions of black and organic carbon aerosol from energy-related combustion, 1850–2000. *Global Biogeochem. Cycles*, **21**, GB2018, doi:10.1029/2006GB002840.
- Charlson, R. J., S. E. Schwartz, J. M. Hales, R. D. Cess, J. A. Coakley Jr., J. E. Hansen, and D. J. Hofmann, 1992: Climate forcing by anthropogenic aerosols. *Science*, **255**, 423–430, doi:10.1126/science.255.5043.423.
- Cherchi, A., A. Alessandri, S. Masina, and A. Navarra, 2011: Effects of increased CO<sub>2</sub> levels on monsoons. *Climate Dyn.*, **37**, 83–101, doi:10.1007/s00382-010-0801-7.
- Collins, W. J., and Coauthors, 2011: Development and evaluation of an Earth-System model—HadGEM2. *Geosci. Model Dev.*, **4**, 1051–1075, doi:10.5194/gmd-4-1051-2011.
- Cook, J., and E. J. Highwood, 2004: Climate response to tropospheric absorbing aerosols in an intermediate general-circulation model. *Quart. J. Roy. Meteor. Soc.*, **130**, 175–191, doi:10.1256/qj.03.64.
- Dash, S. K., M. A. Kulkarni, U. C. Mohanty, and K. Prasad, 2009: Changes in the characteristics of rain events in India. *J. Geophys. Res.*, **114**, D10109, doi:10.1029/2008JD010572.
- D’Errico, M., C. Cagnazzo, P. G. Fogli, W. K. M. Lau, J. von Hardenberg, F. Fierli, and A. Cherchi, 2015: Indian monsoon and the elevated-heat-pump mechanism in a coupled aerosol–climate model. *J. Geophys. Res.*, **120**, 8712–8723, doi:10.1002/2015JD023346.
- Diehl, T., A. Heil, M. Chin, X. Pan, D. Streets, M. Schultz, and S. Kinne, 2012: Anthropogenic, biomass burning, and volcanic emissions of black carbon, organic carbon, and SO<sub>2</sub> from 1980 to 2010 for hindcast model experiments. *Atmos. Chem. Phys.*, **12**, 24 895–24 954, doi:10.5194/acpd-12-24895-2012.
- Dong, B., J. M. Gregory, and R. T. Sutton, 2009: Understanding land–sea warming contrast in response to increasing greenhouse gases. Part I: Transient adjustment. *J. Climate*, **22**, 3079–3097, doi:10.1175/2009JCLI2652.1.
- Ekman, A. M. L., 2014: Do sophisticated parameterizations of aerosol–cloud interactions in CMIP5 models improve the representation of recent observed temperature trends? *J. Geophys. Res.*, **119**, 817–832, doi:10.1002/2013JD020511.
- Fan, F. X., M. E. Mann, S. Lee, and J. L. Evans, 2010: Observed and modeled changes in the South Asian summer monsoon over the historical period. *J. Climate*, **23**, 5193–5205, doi:10.1175/2010JCLI3374.1.
- Fasullo, J., 2012: A mechanism for land–ocean contrasts in global monsoon trends in a warming climate. *Climate Dyn.*, **39**, 1137–1147, doi:10.1007/s00382-011-1270-3.
- Forster, P., and Coauthors, 2007: Changes in atmospheric constituents and in radiative forcing. *Climate Change 2007: The Physical Science Basis*, Cambridge University Press, 130–234. [Available online at <https://www.ipcc.ch/pdf/assessment-report/ar4/wg1/ar4-wg1-chapter2.pdf>.]
- Ganguly, D., P. J. Rasch, H. Wang, and J.-H. Yoon, 2012: Climate response of the South Asian monsoon system to anthropogenic aerosols. *J. Geophys. Res.*, **117**, D13209, doi:10.1029/2012JD017508.
- Gautam, R., N. C. Hsu, K. M. Lau, and M. Kafatos, 2009: Aerosol and rainfall variability over the Indian monsoon region: Distributions, trends and coupling. *Ann. Geophys.*, **27**, 3691–3703, doi:10.5194/angeo-27-3691-2009.
- Goswami, B. N., V. Venugopal, D. Sengupta, M. S. Madhusoodanan, and P. K. Xavier, 2006: Increasing trend of extreme rain events over India in a warming environment. *Science*, **314**, 1442–1445, doi:10.1126/science.1132027.
- Guo, L., A. G. Turner, and E. J. Highwood, 2015: Impacts of 20th century aerosol emissions on the South Asian monsoon in the CMIP5 models. *Atmos. Chem. Phys.*, **15**, 6367–6378, doi:10.5194/acp-15-6367-2015.
- Hurrell, J. W., J. J. Hack, D. Shea, J. M. Caron, and J. Rosinski, 2008: A new sea surface temperature and sea ice boundary dataset for the Community Atmosphere Model. *J. Climate*, **21**, 5145–5153, doi:10.1175/2008JCLI2292.1.
- Johns, T. C., and Coauthors, 2003: Anthropogenic climate change for 1860 to 2100 simulated with the HadCM3 model under updated emissions scenarios. *Climate Dyn.*, **20**, 583–612, doi:10.1007/s00382-002-0296-y.
- Jones, A., D. L. Roberts, M. J. Woodage, and C. E. Johnson, 2001: Indirect sulphate aerosol forcing in a climate model with an interactive sulphur cycle. *J. Geophys. Res.*, **106**, 20 293–20 310, doi:10.1029/2000JD000089.
- Kaskaoutis, D. G., R. P. Singh, R. Gautam, M. Sharma, P. G. Kosmopoulos, and S. N. Tripathi, 2012: Variability and trends of aerosol properties over Kanpur, northern India using AERONET data (2001–10). *Environ. Res. Lett.*, **7**, 024003, doi:10.1088/1748-9326/7/2/024003.
- Kim, M., W. K. M. Lau, K. Kim, J. Sang, Y. Kim, and W. Lee, 2015: Amplification of ENSO effects on Indian summer monsoon by absorbing aerosols. *Climate Dyn.*, **46**, 2657–2671, doi:10.1007/s00382-015-2722-y.
- Kitoh, A., H. Endo, K. Krishna Kumar, I. F. A. Cavalcanti, P. Goswami, and T. Zhou, 2013: Monsoons in a changing world: A regional perspective in a global context. *J. Geophys. Res.*, **118**, 3053–3065, doi:10.1002/jgrd.50258.

- Krishnamurthy, V., and B. N. Goswami, 2000: Indian monsoon–ENSO relationship on interdecadal timescale. *J. Climate*, **13**, 579–595, doi:10.1175/1520-0442(2000)013<0579:IMEROI>2.0.CO;2.
- Krishnan, R., and Coauthors, 2013: Will the South Asian monsoon overturning circulation stabilize any further? *Climate Dyn.*, **40**, 187–211, doi:10.1007/s00382-012-1317-0.
- Lau, K.-M., and K.-M. Kim, 2006: Observational relationships between aerosol and Asian monsoon rainfall, and circulation. *Geophys. Res. Lett.*, **33**, L21810, doi:10.1029/2006GL027546.
- , M. K. Kim, and K. M. Kim, 2006: Asian summer monsoon anomalies induced by aerosol direct forcing: The role of the Tibetan Plateau. *Climate Dyn.*, **26**, 855–864, doi:10.1007/s00382-006-0114-z.
- Lau, W., 2014: Desert dust and monsoon rain. *Nat. Geosci.*, **7**, 255–256, doi:10.1038/ngeo2115.
- Levine, R. C., and A. G. Turner, 2012: Dependence of Indian monsoon rainfall on moisture fluxes across the Arabian Sea and the impact of coupled model sea surface temperature biases. *Climate Dyn.*, **38**, 2167–2190, doi:10.1007/s00382-011-1096-z.
- Martin, G. M., and Coauthors, 2011: The HadGEM2 family of Met Office Unified Model Climate configurations. *Geosci. Model Dev.*, **4**, 723–757, doi:10.5194/gmd-4-723-2011.
- Meehl, G. A., J. M. Arblaster, and W. D. Collins, 2008: Effects of black carbon aerosols on the Indian monsoon. *J. Climate*, **21**, 2869–2882, doi:10.1175/2007JCLI1777.1.
- Nigam, S., and M. Bollasina, 2010: “Elevated heat pump” hypothesis for the aerosol–monsoon hydroclimate link: “Grounded” in observations? *J. Geophys. Res.*, **115**, D16201, doi:10.1029/2009JD013800.
- Pan, X., and Coauthors, 2015: A multi-model evaluation of aerosols over South Asia: Common problems and possible causes. *Atmos. Chem. Phys.*, **15**, 5903–5928, doi:10.5194/acp-15-5903-2015.
- Polson, D., M. Bollasina, G. C. Hegerl, and L. J. Wilcox, 2014: Decreased monsoon precipitation in the Northern Hemisphere due to anthropogenic aerosols. *Geophys. Res. Lett.*, **41**, 6023–6029, doi:10.1002/2014GL060811.
- Ramanathan, V., and Coauthors, 2005: Atmospheric brown clouds: Impacts on South Asian climate and hydrological cycle. *Proc. Natl. Acad. Sci. USA*, **102**, 5326–5333, doi:10.1073/pnas.0500656102.
- Ramesh, K. V., and P. Goswami, 2014: Assessing reliability of regional climate projections: The case of Indian monsoon. *Sci. Rep.*, **4**, 4071, doi:10.1038/srep04071.
- Roberts, D. L., and A. Jones, 2004: Climate sensitivity to black carbon aerosol from fossil fuel combustion. *J. Geophys. Res.*, **109**, D16202, doi:10.1029/2004JD004676.
- Roxy, M. K., K. Ritika, P. Terray, R. Murtugudde, K. Ashok, and B. Goswami, 2015: Drying of Indian subcontinent by rapid Indian Ocean warming and a weakening land–sea thermal gradient. *Nat. Commun.*, **6**, 7423, doi:10.1038/ncomms8423.
- Saha, A., S. Ghosh, A. S. Sahana, and E. P. Rao, 2014: Failure of CMIP5 climate models in simulating post-1950 decreasing trend of Indian monsoon. *Geophys. Res. Lett.*, **41**, 7323–7330, doi:10.1002/2014GL061573.
- Schultz, M. G., and Coauthors, 2008: Global wildland fire emissions from 1960 to 2000. *Global Biogeochem. Cycles*, **22**, GB2002, doi:10.1029/2007GB003031.
- Shindell, D. T., A. Voulgarakis, G. Faluvegi, and G. Milly, 2012: Precipitation response to regional radiative forcing. *Atmos. Chem. Phys.*, **12**, 6969–6982, doi:10.5194/acp-12-6969-2012.
- Smith, S. J., H. Pitcher, and T. M. L. Wigley, 2001: Global and regional anthropogenic sulfur dioxide emissions. *Global Planet. Change*, **29**, 99–119, doi:10.1016/S0921-8181(00)00057-6.
- Sperber, K. R., H. Annamalai, I.-S. Kang, A. Kitoh, A. Moise, A. Turner, B. Wang, and T. Zhou, 2013: The Asian summer monsoon: An intercomparison of CMIP5 vs. CMIP3 simulations of the late 20th century. *Climate Dyn.*, **41**, 2711–2744, doi:10.1007/s00382-012-1607-6.
- Turner, A. G., and H. Annamalai, 2012: Climate change and the South Asian summer monsoon. *Nat. Climate Change*, **2**, 587–595, doi:10.1038/nclimate1495.
- Twomey, S., 1977: The influence of pollution on the shortwave albedo of clouds. *J. Atmos. Sci.*, **34**, 1149–1152, doi:10.1175/1520-0469(1977)034<1149:TIOPOT>2.0.CO;2.
- Ueda, H., A. Iwai, K. Kuwako, and M. E. Hori, 2006: Impact of anthropogenic forcing on the Asian summer monsoon as simulated by eight GCMS. *Geophys. Res. Lett.*, **33**, L06703, doi:10.1029/2005GL025336.
- Vinoj, V., P. J. Rasch, H. Wang, J.-H. Yoon, P.-L. Ma, K. Landu, and B. Singh, 2014: Short-term modulation of Indian summer monsoon rainfall by West Asian dust. *Nat. Geosci.*, **7**, 308–314, doi:10.1038/ngeo2107.
- Wilcox, L. J., E. J. Highwood, and N. J. Dunstone, 2013: The influence of anthropogenic aerosol on multi-decadal variations of historical global climate. *Environ. Res. Lett.*, **8**, 024033, doi:10.1088/1748-9326/8/2/024033.
- Xavier, P. K., C. Marzin, and B. N. Goswami, 2007: An objective definition of the Indian summer monsoon season and a new perspective on the ENSO–monsoon relationship. *Quart. J. Roy. Meteor. Soc.*, **133**, 749–764, doi:10.1002/qj.45.